Arch. Metall. Mater. **66** (2021), 1, 197-203

DOI: 10.24425/amm.2021.134776

CHUNZHI XIA[1*], LINLING FU[1], WENCHAO DU[1], XIANGPING XU[1],
XILING WANG[2], JIASHENG ZOU[1]

THERMAL FATIGUE DAMAGE AND RESIDUAL MECHANICAL PROPERTIES OF WCu45/FeCr18Ni9 STEEL BRAZED JOINT WITH NiCrSiBFe FILLER METAL

Thermal fatigue properties of WCu45/FeCr18Ni9 steel brazed joint with Ni-Cr-Si-B filler metal were investigated. Results indicated that the fatigue damage of Ni-based joint was aggravated with the increased of thermal fatigue cycles times. Moreover, the fatigue cracks appeared in the brazing seam and FeCr18Ni9 steel side near the brazing seam, and the bending strength of the brazed joint decreased from 333 MPa of original joint to 160 MPa of having experienced 200 thermal fatigue cycles. The fracture characteristic of Ni-based joint underwent 200 cycles was identified as mixed ductile-brittle fracture under the combined effect of external bending load and internal fatigue damage.

Keywords: Ni-based brazed joint, Thermal fatigue damage, Residual mechanical properties, Fracture morphology

1. Introduction

W-Cu alloy is a very promising material for its excellent conductive and thermal conductivity, high temperature strength, low coefficient of thermal expansion and good resistance arc erosion resistance [1-3]. Owing to these properties, it is a kind of high temperature composite material with great development potential. However, unfavorable low temperature toughness and poor high temperature oxidation resistance of the W-Cu composite constrained its application in high temperature condition corrosive environments. Fabrication of the W-Cu composite component by means of dissimilar materials, can expand application the range of the W-Cu composites by making full use of the advantages of two types of materials.

Thermal fatigue was an important index of service life of the W alloy joint. Damage and fatigue crack growth of Eurofer97(a ferritic/martensitic 9Cr steel) steel first wall mock-up under cyclic heat flux loads was investigated by J.H. You [4]. B.A. Kalin presented the joints of W with W and monocrystalline W with Eurofer97 steel with Ti–V–Cr–Be and Fe–Ta–Ge–Si–B–Pd filler metal, respectively. No brazed joints with monocrystalline W have been broken during the thermocycling tests [5]. The Japan Atomic Energy Research Institute has developed divertor mock-ups coated with tungsten using the chemical vapor deposition technique. Experiments were carried out in an electron beam gun facility to evaluate the thermal fatigue and critical performances of the CVD-W layer. Thermal fatigue tests showed that both mock-ups successfully withstood a steady-state deposited heat flux of 5 MW/m^2 for 1000 cycles [6]. X. Liu has joined W/CuCrZr by low activation Cu–Mn filler metal. Thermal fatigue test indicated that brazed W/CuCrZr mockups could withstand 8 MW/m^2 heat flux for 1000 cycles without visible damages [7].

Previous efforts have investigated vacuum brazed WCu45 alloy and FeCr18Ni9 with Ag-based, Cu-based and Ni-based brazing alloy. FeCr18Ni9 is an austenitic steel with Cr, Ni and C as major alloying elements, which also might be marked as SUS302 or 1Cr18Ni9. Ag-based [8] and Cu-based [9] brazing joints exhibited favorable plastic deformation ability and high bending strength. Ni-based [10] filler metal has excellent performance at high temperature and superior wettability to the WCu45 alloy. This paper demonstrated microstructure, residual mechanical properties and fracture morphology of Ni-based joint with difference fatigue cycles times to reveal Ni-based brazed joint thermal fatigue performance.

[1] JIANGSU UNIVERSITY OF SCIENCE AND TECHNOLOGY, SCHOOL OF MATERIALS SCIENCE AND ENGINEERING, ZHENJIANG, 212003, CHINA
[2] JIANGSU JIAOTONG COLLEGE, DEPARTMENT OF AEROSPACE, ZHENJIANG, 212028, CHINA

* Corresponding author: cz_xia@126.com

© 2020. The Author(s). This is an open-access article distributed under the terms of the Creative Commons Attribution-NonCommercial License (CC BY-NC 4.0, https://creativecommons.org/licenses/by-nc/4.0/deed.en which permits the use, redistribution of the material in any medium or format, transforming and building upon the material, provided that the article is properly cited, the use is noncommercial, and no modifications or adaptations are made.

2. Materials and Methods

2.1. Materials

In this research, WCu45 alloy (contained 45wt% of Cu) and FeCr18Ni9 steel were used as the base materials, and NiCrSiBFe alloy was used as a filler metal. The chemical compositions of FeCr18Ni9 steel and NiCrSiBFe brazing filler metal, are listed in Table 1. WCu45 alloy and FeCr18Ni9 steel were cut by a linear cutting machine into blocks with sizes of 20×20×5 mm. NiCrSiBFe filler metal was prepared in the form of foil with a thickness of 0.05 mm.

2.2. Brazing

Before being brazed, oxides and greasy dirt on the surface of the base metals and the filler metal were eliminated by using emery papers and then cleaned by ultra-sonication in alcohol for 15 minutes. Subsequently, the samples were assembled, in the sequence of WCu45 alloy, brazing filler metal and FeCr18Ni9 steel in a special clamp, as schematically illustrated in Fig. 1.

Moreover, suitable pressure was imposed on the surface of WCu45 alloy, with the purpose of promoting the brazing filler metal to spread out and wet adequately on the base metals, and using a stainless steel spacer of 0.02 mm to control the brazing clearance accurately. Then the clamp and the samples in the clamp were placed together into a vacuum furnace for brazing under the given process parameters (as shown in Table 2).

2.3. Thermal fatigue test

After the brazing process, samples were cut by a linear cutting machine into blocks with sizes of 40×6×5 mm from the brazed joint, and a circular hole with a diameter of 5 mm was drilled on the FeCr18Ni9 steel at a distance of 15mm away from the brazing seam (Fig. 2). Moreover, the samples were exposed to thermo cycling tests as follows: 0, 100, 150 and 200 cycles of heating to 400°C for 20 min, then cooling by water for 2 min.

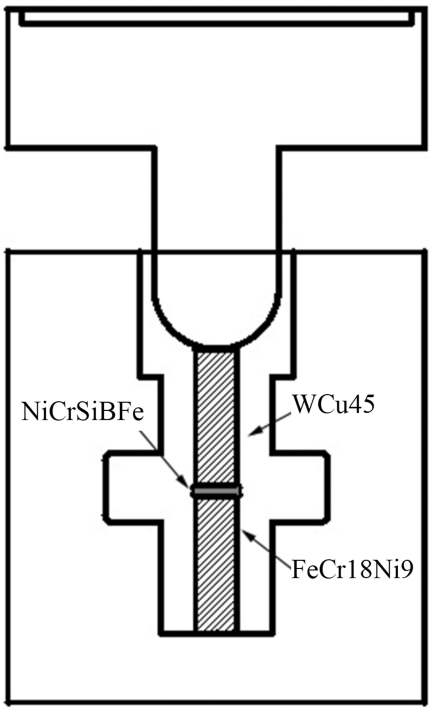

Fig. 1. Sketch of the clamp used in the brazing process

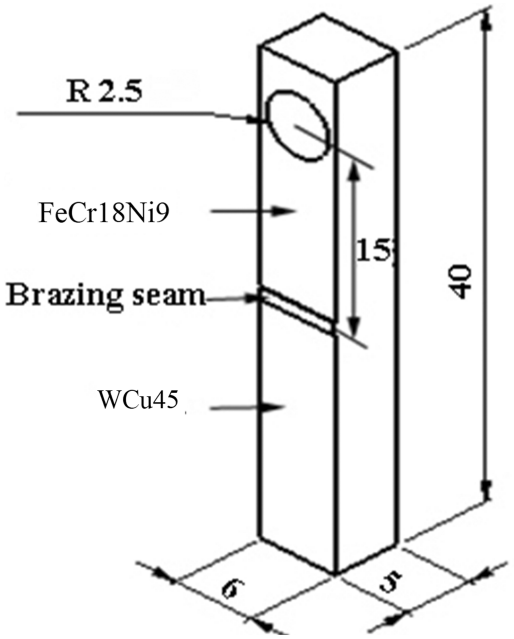

Fig. 2. Thermal fatigue specimen

TABLE 1

Chemical compositions of FeCr18Ni9 steel and brazing filler metals

Materials	Chemical compositions (wt%)										
	C	Cr	Ni	Si	Mn	S	P	B	Fe	Co	Ti
FeCr18Ni9	0.018	17.50	9.27	0.59	0.97	0.0043	0.0287	—	Bal.	0.14	0.13
NiCrSiBFe	—	7.5	Bal.	4.5	—	—	—	2.8	2.5	—	—

TABLE 2

Process parameters of brazing

Brazing filler metals	Brazing temperature T/°C	Hold time t/min	Vacuum level /Pa	Brazing clearance /mm
NiCrSiBFe	1060	30	$<6\times10^{-3}$	0.02

2.4. Other test

After the thermal fatigue test, samples were ground with a series of different types of emery papers, polished, and finally etched with a mixed solution of H_2O, HCl, and $CuSO_4$ (50 ml:50 ml:10 g) for 10-20 s. Microstructural feature and fracture morphology of the brazed joint after different cycle times were observed by scanning electron microscope (JSM6480) and energy dispersive spectrum (EDS), and the four-point bending strength of the brazed joints after different cycle times was tested using an electronic mechanical testing machine (CMT5205).

3. Results and discussion

3.1. Microstructure thermal fatigue damage

Fig. 3 illustrates the microstructure of WCu45/NiCrBSiFe/FeCr18Ni9 brazed joint with difference fatigue cycles. The original joint (Fig. 3(a)) formed a good metallurgical combination with a width of about 0.05 mm, and an obvious diffusion layer existed in the brazing seam region near WCu45 alloy side. A smooth and clear bonding interface was formed, without obvious defects such as pores and microcracks appeared. A quantitative overview of the chemical analysis for the different areas was listed in Table 3. According to the binary phase diagram of Fe-Ni, Cr-Ni, and Ni-W [11], the main phase of the brazing seam was γ-Ni solid solution, which dissolved some elements such as W, Cu, Cr and Fe, and a small amount of silicide was obtained in the center of brazing seam.

TABLE 3

Chemical compositions of representative areas of WCu45/ FeCr18Ni9 steel brazed joint

Characteristic region	Ni	Cr	Si	Fe	Cu	W
A	32.21	21.90	—	45.89	—	—
B	49.55	10.40	—	—	15.74	24.31
C	76.88	7.32	2.05	5.60	8.15	—
D	45.19	15.73	13.50	18.10	7.48	—
E	9.57	18.94	1.27	70.22	—	—

A fatigue crack with a length of about 0.02 mm appeared in the center of the brazing seam after 100 fatigue cycles demonstrated by Fig. 3(b). Upon the EDS analysis, the D point of crack initiation was mainly consisted of Ni 45.19%, Cr 15.73%, Si 13.50%, Fe 18.10% and Cu 7.48% (wt.%).According to the binary phase diagram of Ni-Si, some silicide was formed (as shown in D zone of Fig. 3(b)).

The γ-Ni based solid solution continued to product dislocations under the effect of thermal stress. Due to the ability of the silicide and boride in the brazing seam to produce disloca-

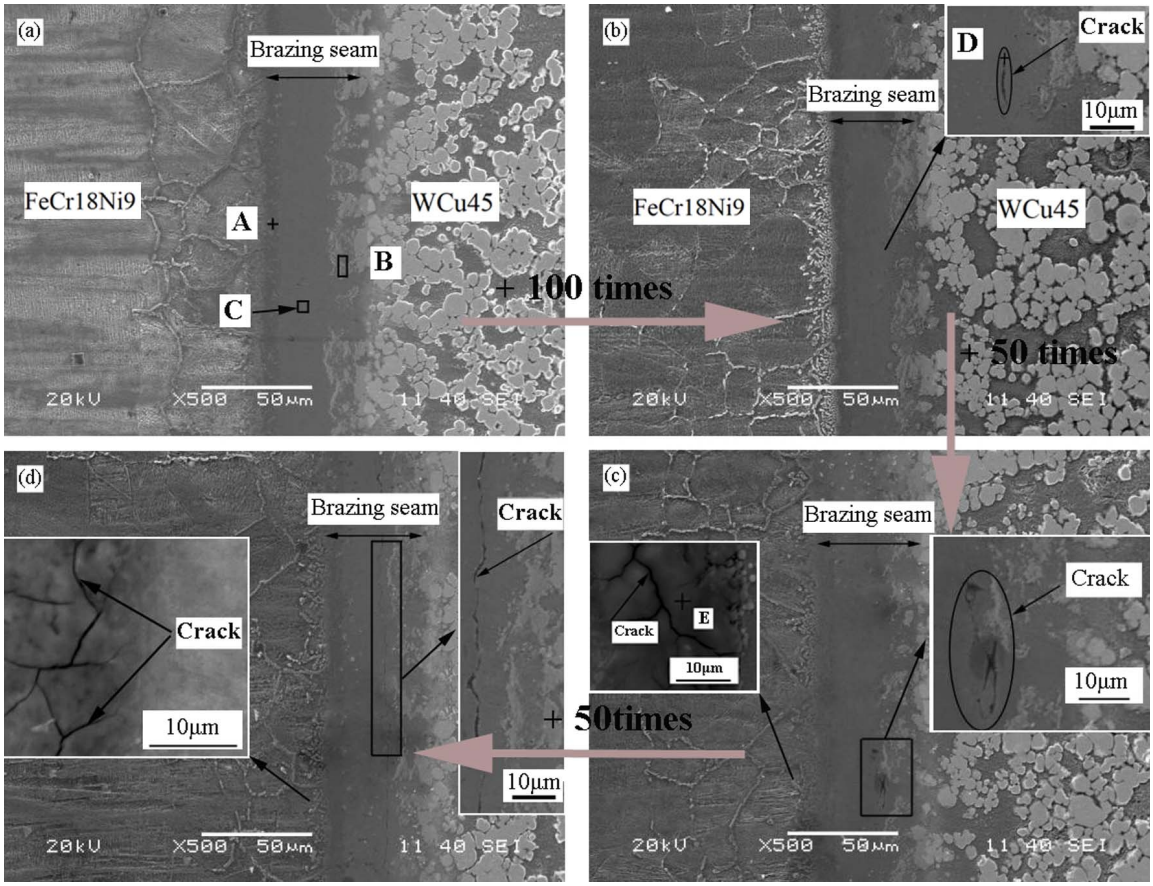

Fig. 3. Microstructure of the WCu45/FeCr18Ni9 steel brazed with difference fatigue cycles: (a) Original joint; (b) 100 fatigue cycles; (c) 150 fatigue cycles; (d) 200 fatigue cycles

tions was limited, the movement of dislocations on slip plane to a certain extent would be blocked and piled up, resulting in stress concentration. The silicide and boride in the brazing seam cracked first when thermal stress added up to a certain value, and fatigue cracks propagated along grain boundaries because of grain boundary weakness at upper temperature of 400°C during the fatigue crack test.

The number of fatigue cracks was increased compared with former, two intersecting cracks was presented in the brazing seam after 150 fatigue cycles. Meanwhile, there were multiple cracks appeared in the FeCr18Ni9 steel near the brazing seam, as depicted in Fig. 3(c). In the vicinity of the main crack continued to sprout small cracks under thermal stress, and the main cracks and the small cracks propagated along the grain boundaries were finally connected. Moreover, fatigue damage appeared in the FeCr18Ni9 steel near brazing seam side for the high coefficient of thermal expansion at both sides of the grain boundary. The microstructure of WCu45/FeCr18Ni9 steel brazed joint with NiCrSiBFe filler metal after 200 cycles was shown in Fig. 3(d). It could be seen that a long crack was distributed longitudinally in the brazing seam. Meanwhile, a number of cracks were observed on the FeCr18Ni9 steel, and the cracks were connected with each other to form a grid.

When the main crack grew along the crystal, the stress concentration at the other small crack tip would be reduced. Therefore, the crack propagation rate would decrease or terminate, leading to a very long main crack, while the other small cracks was short. The austenite grain boundary was weakened serious after 200 fatigue cycles, then the crack continued to expand along the austenite grain boundary, and finally the crack mesh was formed.

In summary, with the increased of thermal fatigue cycles, fatigue cracks occurred in the brazing seam and FeCr18Ni9 steel. The cracks in the brazing seam were induced in the silicide and boride, and cracks in the FeCr18Ni9 steel were induced at austenite grain boundaries. The crack propagation paths were intergranular, and the diagram of microstructure after thermal fatigue damage of WCu45/FeCr18Ni9 steel brazed joint was presented in Fig. 4.

3.2. Residual mechanical properties

3.2.1. Four-point bending strength

Residual mechanical properties of the brazed joint with different cycle times was evaluated using the four-point bending strength at room temperature. The dimensional size of bending test samples were 40× 6× 5 mm and tested on an electronic mechanical testing machine (CMT5205) using a special fixture with a cross-head speed of 0.5 mm/min. Five bending test samples were prepared for the four-point bending test of each cycle times. From a load-displacement curve, the bending strength (σ) was calculated by the following formula:

$$\sigma = \frac{3Fl}{bh^2} \tag{1}$$

In this formula, F is the average maximum load, l is the distance between two effect points, and b (mm) and h (mm) are the specimen width and thickness, respectively. The four-point bending strength of original joint was about 333MPa after the calculation. However, the residual mechanical four-point bending strength only 160MPa after 200 fatigue cycles times. Fig. 5 depicted the four-point bending strength with difference cycles times.

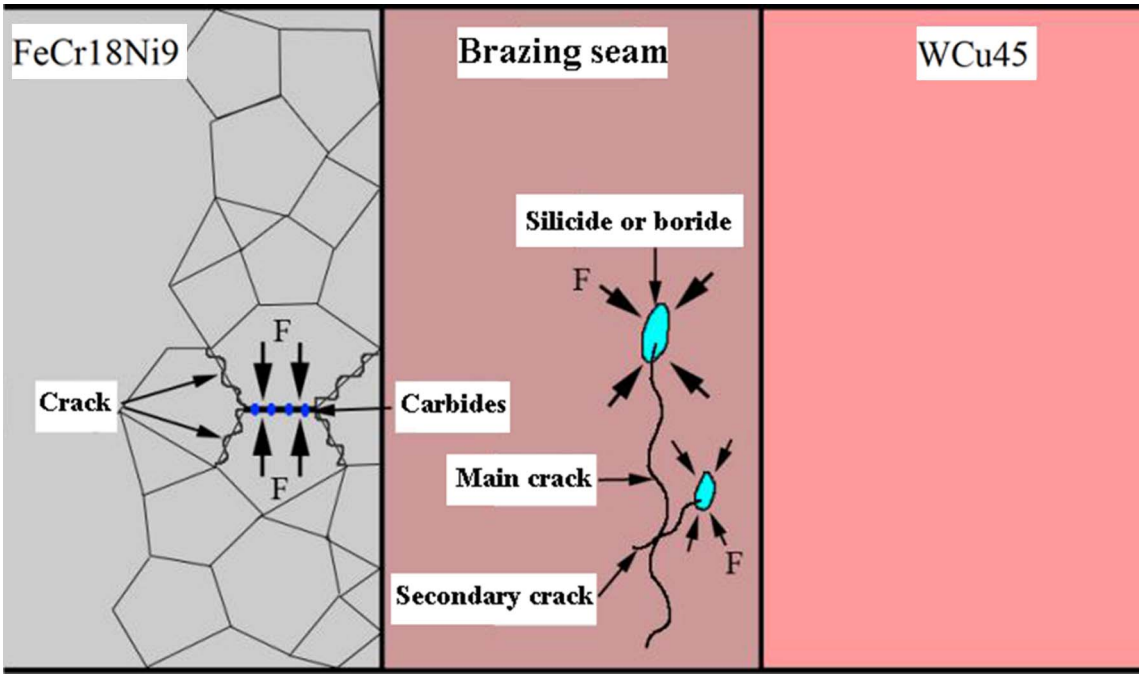

Fig. 4. The diagram of thermal fatigue damage of WCu45/FeCr18Ni9 steel brazed joint

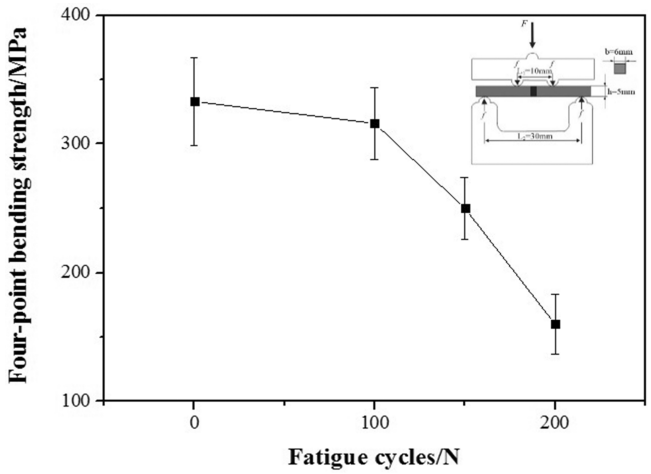

Fig. 5. The four-point bending strength with difference cycles times

3.2.2. Fracture morphology

Fracture morphology analysis of the brazed joint was an important link with the analysis of mechanical properties of joints. Therefore, the bending fracture of WCu45/FeCr18Ni9 steel brazed joint after thermal fatigue test was analyzed. Fig. 6 depictes the SEM morphologies of the four-point bending fracture surface of the brazed joints. It could be seen that the original macro section were darker and relatively flat. Meanwhile, some holes were scattered in macro surface. Those small holes were formed by tearing during loading. Meanwhile, the micro section presented the fracture features were partial cleavage step and dimple topography. There were obvious tear edges near the dimple grain boundary, and the inner part of the dimple was distributed with blocky structure. The EDS spectrometer

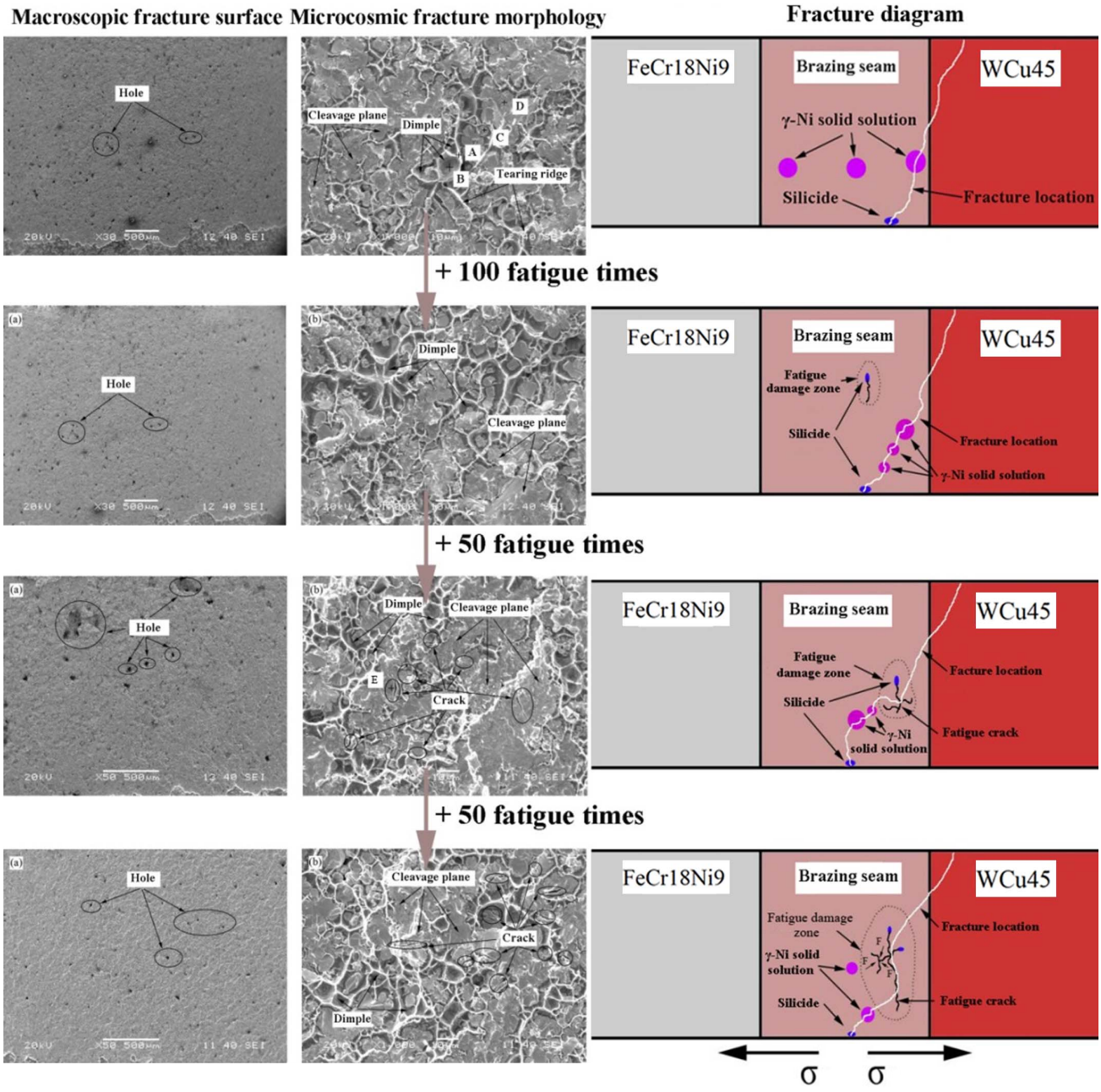

Fig. 6. Fracture morphology and fracture diagram with difference fatigue cycles

was used to analyze the position of A, B, C and D in Fig. 6, and results are listed in Table 4. It could be illustrated that the torn edges (feature A) consisted of Ni (Cu) solid solution and a small amount of silicide, the internal dimple (feature B) was Ni (Cu) solid solution, and the mass of tissue (area C) and cleavage plane (area D) were mainly fracture morphology of WCu45 alloy.

TABLE 4

Composition in the representative areas of Ni-based fracture surface before thermal fatigue test

Characteristic region	Ni	Cu	W	Si	Fe
A	41.01	55.87	—	3.12	—
B	43.75	56.25	—	—	—
C	—	11.97	88.03	—	—
D	—	19.85	80.15	—	—
E	41.26	54.14	—	3.15	1.45

During the bending test of Ni-brazed joints, the crack appeared first at the region of hard phase because the plasticity of this type phase was worse than that of the solid solution in the brazing joint. The bending loads would produce a large number of dislocations because of Ni (Cu) solid solution's good plasticity. When the bending load up to a certain extent, micro holes was first formed in Ni-(Cu) solid solution. A large number of dislocations gathered under the action of bending stress to the microscopic cavity, which made the cavity grew up. The cavities grew together and connected with each other to form dimples. The interior of the dimple contained a block of WCu45 base material, and it may be the cross-sectional morphology of the joint surface between the brazing seam and the WCu45 base metal. The W skeleton would be stripped off first to form a large smooth cleavage surface due to the lack of sufficient plasticity. Therefore, the bending fracture characteristics of WCu45/FeCr18Ni9 original joint was identified as mixed ductile-brittle fracture, ductile fracture occurred in the joint of Ni based solid solution, and brittle fracture occurred at the WCu45 base metal.

The bending fracture morphology of WCu45/FeCr18Ni9 brazed joint subjected to 100 cycles was similar to the original joint. And there were many voids left in the macro section. Meanwhile, the microstructure of the micro cross section was mainly dimples and cleavage plane, and the overall fracture was ductile brittle fracture mode. 100 thermal fatigue cycle did not cause obviously internal damage to the joint, and the Ni-based joint was mainly subjected to the external bending load before the fracture failure occurring. During the bending test, the silicide at the bottom of the seam would crack first because of the strong tensile stress at the bottom of the brazed joint. As the bending load increased, the crack expanded rapidly from bottom to top along the brittle region of the joint. No obvious cracks were observed on the micro section, and the final fracture position of the joint was different from the region of thermal fatigue damage. It could also reflected that the fracture characteristics of Ni based joints were consistent with thermal fatigue tests after 100 cycles.

After 150 thermal fatigue cycles, the larger dimension of the brazed joint was found on the macro section, which showed that the tearing of the base metal was more obvious. Furthermore, the micro morphology was still dominated by dimples and cleavage plane, and several small cracks were distributed on the micro section of the brazing seam. The components of the small cracks were analyzed by EDS spectrometer (Table 4). The location of the crack distribution (characteristic area E) had a small amount of silicide. Moreover, the dimples were mainly Ni based solid solutions, and the cleavage planes were WCu45 alloy. There were several small cracks in the micro section, which indicated that the joint had been damaged to some extent before bending test. The fatigue crack initiated at the hard region in the brazing seam under the action of thermal stress. Subsequently, the fatigue crack expanded rapidly, and it caused new small cracks under the action of bending stress. Above all, the cross section of the brazed joint underwent 150 fatigue cycles was formed under the combined action of the external bending load and the internal thermal fatigue damage. The fracture features were ductile brittle mixed fracture.

There was holes distributed with cross section after 200 thermal fatigue times, those holes were left by the tearing of the base material. Moreover, the overall change was little compared with the previous ones. In addition to the same dimple and cleavage surface morphology, there were more small cracks in the micro section than the previous joint section.

Small fatigue cracks could be observed everywhere on the microscopic section, which indicated that a large number of fatigue crack initiated and propagated in the joint were existed before the joint subjected to the external bending load. On the one hand, the main crack at the bottom of the brazing seam rapidly expanded to the fatigue crack, and on the other hand, bending stress continuously produced stress concentration at the tip of the fatigue crack. The interaction between the main crack and a large number of small fatigue cracks leaded to the final fracture. The influence of strength of the brazed joints decreased considerably after 200 cycles, which reflected the extent of thermal fatigue damage. Therefore, the cross section of the brazed joint underwent 200 fatigue cycles was the bending load formed on the basis of thermal fatigue damage. The fracture features were ductile and brittle mixed fracture.

4. Conclusions

(1) The original joint showed a smooth and clear bonding interface without obvious micro holes, cracks, and other microdefects. Micro crack initiation on hard region and propagation along grain boundaries in brazing seam after 100 cycles, and cracks appeared in the brazing seam and FeCr18Ni9 steel side near the brazing seam after the brazed joint underwent 150 fatigue cycles. There was a long crack in the seam and a crack mesh appeared in the FeCr18Ni9

steel side near the brazing seam as the fatigue cycles increased, which indicated that the joint was subjected to more severe fatigue damage.

(2) The four-point bending strength of the brazed joint decreased with the increment of the fatigue cycles. In addition, fracture morphology illustrated that the fatigue damage became more obvious as the fatigue cycles increased. Meanwhile, the fracture feature was coincident with difference cycles. They were identified as mixed ductile-brittle fracture under the combined action of external bending load and interior fatigue damage.

Acknowledgment

This project was supported by the National Natural Science Foundation of China (Grant No.51405205), and the Project Funded by China Postdoctoral Science Foundation (2015M581751).

REFERENCES

[1] M.H. Maneshian, A. Simchi, Z.R. Hesabi, Mat. Sci. Eng. A. **445** (6), 86-93 (2007).

[2] Y.D. Kim, N.L. Oh, S.T. Oh, I.H. Moon, Mater. Lett. **51** (5), 420-424 (2001).

[3] J.C. Koh, A. Fortini, Int. J. Heat Mass Transfer. **16** (11), 2013-2022 (1973).

[4] J.H. You, T. Höschen, G. Pintsuk, Fusion Eng. Des. **89** (4), 284-288 (2014).

[5] B.A. Kalin, V.T. Fedotov, O.N. Sevrjukov, A.N. Kalashnikov, A.N. Suchkov, A. Moeslang, M. Rohde, J. Nucl. Mater. **367** (4), 1218-1222 (2007).

[6] J. Boscary, S. Suzuki, K. Nakamura, T. Suzuki, M. Akiba, Fusion Eng. Des. **39–40** (98), 537-542 (1998).

[7] X. Liu, Y.Y. Lian, L. Chen, Z.K. Cheng, J.M. Chen, X.R. Duan, J.P. Song, Y. Yu, J. Nucl. Mater. **455** (1-3), 382-386 (2014).

[8] C.Z. Xia, Q.H. Liang, J.S. Zou, X.P. Xu, High Temp. Mater. Pr. **33** (3), 293-298 (2013).

[9] C.Z. Xia, Q.H. Liang, X.P. Xu, J.S. Zou, Sci. Eng. Comp. Mater. **22** (3), 245-250 (2015).

[10] C.Z. Xia, J. Yang, J.S. Zou, X.P. Xu, Kovove Mater. **54**, 1-7 (2016).

[11] N. Seizo, H. Makoto, Binary alloy phase diagram, Metallurgical Industry, Beijing (2004).